VNU Journal of Science: Mathematics – Physics, Vol. 34, No. 4 (2018) 9-18

VNU Journal of Science: Mathematics - Physics

Journal homepage: https://js.vnu.edu.vn/MaP

Effective Excess Charge Density in Water Saturated Porous Media

Luong Duy Thanh*

Thuy Loi University, 175 Tay Son, Dong Da, Ha Noi, Vietnam

Received 03 October 2018
Revised 28 OCtober 2018; Accepted 01 November 2018

Abstract: A model for the effective excess charge in a capillary as well as in porous media is developed for arbitrary pore scales. The prediction of the model is then compared with another published model that is limited for a thin electric double layer (EDL) assumption. The comparison shows that there is a deviation between two models depending on the ratio of capillary/pore radius and the Debye length. The reasons for the deviation between two models are not only due to the thin EDL assumption to get electrical potential and charge distribution in pores but also to some other approximations for integral evaluations. The results suggest that the model developed in this work can be used with arbitrary capillary/pore scale and thus is not restricted to the thin EDL assumption.

Keywords: Zeta potential, porous media, electric double layer, effective excess charge.

1. Introduction

The self-potential (SP) method is a passive geophysical method based on the measurements of the natural electrical potentials at the ground surface of the Earth. The SP survey has the advantage of being non-destructive, fast, inexpensive and very simple to perform in the field requiring only a high impedance millivoltmeter and at least two non-polarizable electrodes connected through a reel of wire. The SP method has been used for a variety of geophysical applications. For example, the SP measurements could be used to characterize active volcanic areas [1, 2], to detect and monitor ground-water flow [3, 4], contaminant plumes [5, 6] or to study landslides [7, 8]. In natural porous media, several main mechanisms proposed to explain SP signals are associated with streaming potential, electrochemical, thermoelectric, redox, or piezoelectric effects [9]. An overview of other possible mechanisms is available in [e.g., 10].

In this work, the SP signal that is often referred to as streaming potential due to the water flow in porous media is considered. The surface of the minerals that constitute porous media is generally

*Tel.: 84-936946975.
Email: luongduythanh2003@yahoo.com
https//doi.org/ 10.25073/2588-1124/vnumap.4294

electrically charged, creating an electrical double layer (EDL) containing an excess of charge that counterbalances the charge deficiency of the mineral surface [11, 12]. Fig. 1 shows structure of the EDL: a Stern layer that contains only counterions coating the mineral with a very limited thickness and a diffuse layer that contains both counterions and coions but with a net excess charge. The shear plane that can be approximated as the limit between the Stern layer and diffuse layer separates the mobile and immobile part of the water molecules when subjected to a fluid pressure difference. The electrical potential at the shear plane is called the zeta potential (ζ) [11]. In the bulk liquid, the number of cations and anions is equal so that it is electrically neutral. There are two main approaches to model streaming potential in saturated porous media. The first one is based on the use of the coupling coefficient which is a rock-dependent property that relates the hydraulic pressure difference to the electrical potential difference [e.g., 13, 14]. The second one is more recent and focuses on the excess charge that is dragged by the water flow [15-17, 18]. In this approach, the coupling parameter is the excess charge that is effectively dragged by water in the porous media.

Recently, Guarracino and Jougnot (2018) have developed a theoretical model to predict the effective excess charge density in saturated porous media using a bundle of capillary tubes of different radius with a fractal pore-size distribution [19]. They used the thin EDL assumption (i.e., the thickness of the double layer is small compared to the pore size). Their proposed model shows the dependence of the effective excess charge on the electrolyte concentration and microstructure parameters of porous media like porosity, permeability and tortuosity. Their model has been successfully examined by different sets of experimental data.

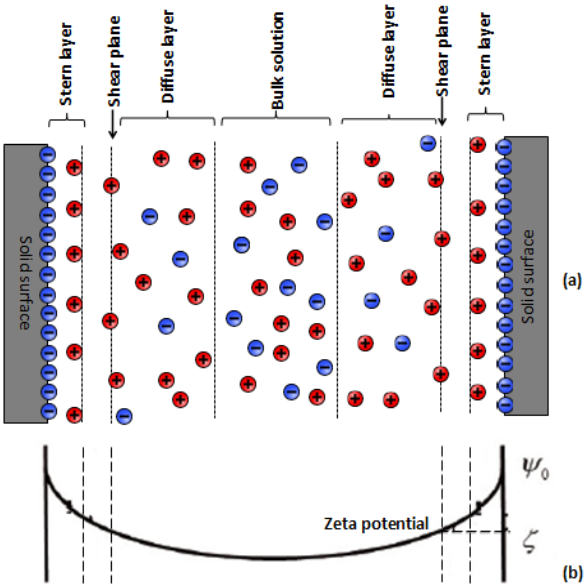

Figure 1. Schematic view of the EDL model. (a) Charge distribution. (b) Electric potential distribution. Figure is modified from [13].

Such a thin EDL assumption, however, is not always satisfied, especially for natural or artificial porous media with low permeability, such as mudstone or shale saturated by low salinity water [20]. Therefore, the model proposed by [19] is not valid for those systems of porous media and water. In this work, a model for the effective excess charge is developed for arbitrary pore scales based on a simpler picture of porous media. Namely, a representative elementary volume (REV) of a porous medium (see

Fig. 2) with the physical length L and cross-sectional area A can be approximated as an array of N parallel capillaries of length L_τ with the same radius r [13]. The prediction from the obtained model is then compared with [19]. The comparison shows that there is a deviation between two models depending on the ratio of capillary/pore radius and the Debye length. The reasons for the deviation between two models are not only due to the thin EDL assumption but also to some other approximations for integral evaluations. The results suggest that the model developed in this work can be used with arbitrary capillary/pore scale and thus is not restricted to the thin EDL assumption.

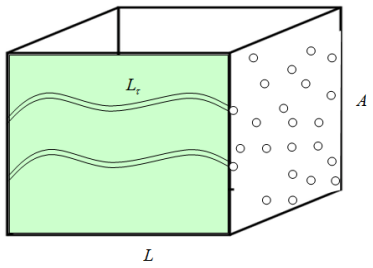

Figure 2. The REV of a porous medium composed of a large number of tortuous capillaries with same radius.

2. Theoretical development

The distribution of the excess charges in the diffuse layer of a capillary is governed by the Poisson-Boltzmann equation [21]:

$$\frac{1}{r}\frac{d}{dr}\left(r\frac{d\psi(r)}{dr}\right)=-\frac{\rho(r)}{\varepsilon_r\varepsilon_0} \quad (1)$$

where $\psi(r)$ and $\rho(r)$ is the electric potential (in V) and the volumetric charge density (in C m^{-3}) in the liquid at the distance r from the axis of the capillary, respectively; ε_r is the relative permittivity of the fluid (78.5 at 25°C for water) and ε_o is the dielectric permittivity in vacuum (8.854×10^{-12} C^2 J^{-1} m^{-1}).

For symmetric electrolytes such as NaCl or $CaSO_4$ in the liquid, $\rho(r)$ is given by [22]

$$\rho(r)=-2N_A eZC_f \sinh\left(\frac{eZ\psi(r)}{k_bT}\right) \quad (2)$$

where C_f is the electrolyte concentration in the bulk fluid representing the number of ions (anion or cation) (mol m^{-3}), e is the elementary charge (e = 1.6×10^{-19} C), Z is the valence of the ions under consideration (dimensionless); k_b is the Boltzmann's constant (1.38×10^{-23} J/K), T is the Kelvin temperature (in K) and N_A is the Avogadro's number (6.022×10^{23}/mol).

Putting Eq. (2) into Eq. (1), one obtains

$$\frac{1}{r}\frac{d}{dr}\left(r\frac{d\psi(r)}{dr}\right)=\frac{2N_A eZC_b}{\varepsilon_r\varepsilon_0}\sinh\left(\frac{eZ\psi(r)}{k_bT}\right) \quad (3)$$

The boundary conditions to be satisfied for the cylindrical capillary surface are: (i) the potential at the surface $r = R$ (R is the radius of the capillary), $\psi(R) = \zeta$; (ii) the potential at the center of the capillary $r = 0$, $\left.\frac{d\psi(r)}{dr}\right|_{r=0} = 0$ [19, 22]

By solving Eq. (3) with the linear approximation ($\sinh(\frac{eZ\psi(r)}{k_bT}) \approx \frac{eZ\psi(r)}{k_bT}$ for small values of $\frac{eZ\psi(r)}{k_bT}$ [23]), the analytical solution of $\psi(r)$ and $\rho(r)$ are obtained as [22]

$$\psi(r) = \zeta \frac{I_o(\frac{r}{\lambda})}{I_o(\frac{R}{\lambda})} \tag{4}$$

$$\rho(r) = -\frac{\varepsilon_r \varepsilon_0 \zeta}{\lambda^2} \frac{I_o(\frac{r}{\lambda})}{I_o(\frac{R}{\lambda})} \tag{5}$$

where I_o is the zero-order modified Bessel function of the first kind and λ is the Debye length characterizing EDL thickness given by

$$\lambda = \sqrt{\frac{\varepsilon_o \varepsilon_r k_b T}{2N_A Z^2 e^2 C_f}} \tag{6}$$

It should be noted that the electrical potential $\psi(r)$ for a thin EDL assumption is given by [e.g., 19, 23]

$$\psi(r) = \zeta . e^{-\frac{R-r}{\lambda}} \tag{7}$$

By solving the Navier-Stokes equation, the velocity profile of the fluid in a cylindrical capillary with pressure driven is given by [24]

$$v(r) = \frac{\Delta P}{4\eta L_\tau}\left(R^2 - r^2\right) \tag{8}$$

where ΔP is the pressure difference across the capillary, η is the dynamic viscosity of the fluid and L_τ is the real length of the tortuous capillary that is related to the length of the porous media by $L_\tau = L.\tau$ (τ is the tortuosity of the capillary).

The effective excess charge density $\hat{Q}_v^R$ carried by the water flow in a single tube of radius R is defined by [e.g., 19]

$$\hat{Q}_v^R = \frac{1}{v_{av}.\pi R^2} \int_0^R \rho(r).v(r).2\pi r dr \tag{9}$$

where v_{av} is the average velocity in the capillary and that is given by [25]

$$v_{av} = \frac{\Delta P.R^2}{8\eta L_\tau} \tag{10}$$

Putting Eq. (5), Eq. (8) and Eq. (10) into Eq. (9), one obtains:

$$\hat{Q}_v^R = -\frac{4\varepsilon_r \varepsilon_0 \zeta}{R^4.\lambda^2..I_o(\frac{R}{\lambda})}\left[\int_0^R R^2 I_o(\frac{r}{\lambda})rdr - \int_0^R I_o(\frac{r}{\lambda})r^3 dr\right] \tag{11}$$

After evaluating the integral and making arrangements, Eq. (11) is written as

$$\hat{Q}_v^R = \frac{8\varepsilon_r \varepsilon_0 \zeta}{R^2.}\left[\frac{2\lambda}{R}.\frac{I_1(\frac{R}{\lambda})}{I_o(\frac{R}{\lambda})} - 1\right] \tag{12}$$

where I_1 is the first-order modified Bessel function of the first kind.

The effective excess charge density $\hat{Q}_v^{REV}$ carried by the water flow in the REV consisting N capillaries of the same radius R is defined in the same way as mentioned in [19]

$$\hat{Q}_v^{REV} = \frac{\hat{Q}_v^R.N.\pi R^2.v_{av}}{v_D.A} \tag{13}$$

where A is the cross sectional area of the REV (see Fig. 2) and $v_D = \frac{\kappa}{\eta}.\frac{\Delta P}{L}$ is the Darcy velocity (m/s) (κ is the permeability of the porous medium). Eq. (13) is now rewritten as

$$\hat{Q}_v^{REV} = \frac{\hat{Q}_v^R.N.\pi R^2}{A}.\frac{R^2.L}{8\kappa L_\tau} \tag{14}$$

The porosity ϕ of the REV of the porous media is defined as

$$\phi = \frac{V_V}{V_T} \tag{15}$$

where V_V is the volume of void-space ($V_V = N.\pi R^2.L_\tau$) and V_T is the total volume of the REV ($V_T = A.L$). Consequently, the porosity is given by

$$\phi = \frac{V_V}{V_T} = \frac{N.\pi R^2.L_\tau}{A.L} \tag{16}$$

Combining Eq. (12), Eq. (14) and Eq. (16) yields

$$\hat{Q}_v^{REV} = \hat{Q}_v^R.\frac{R^2.\phi}{8\kappa}.\left(\frac{L}{L_\tau}\right)^2 = \hat{Q}_v^R.\frac{R^2.\phi}{8\kappa\tau^2} = \varepsilon_r \varepsilon_0 \zeta\left[\frac{2\lambda}{R}.\frac{I_1(\frac{R}{\lambda})}{I_o(\frac{R}{\lambda})} - 1\right].\frac{1}{\tau^2}\frac{\phi}{\kappa} \tag{17}$$

For the case where porous media made up of the capillaries with the same radius, the permeability of the porous media is given by [e.g., 14]

$$\kappa = \frac{\phi R^2}{8\tau^2} \tag{18}$$

Combining Eq. (6), Eq. (17) and Eq. (18) yields

$$\hat{Q}_v^{REV} = \varepsilon_r \varepsilon_0 \zeta \left[\frac{2}{X} . \frac{I_1(X)}{I_o(X)} - 1 \right] . \frac{1}{\tau^2} \frac{\phi}{\kappa} \tag{19}$$

$$\text{where } X = \frac{R}{\lambda} = \sqrt{\frac{16\tau^2 \kappa N_A Z^2 e^2 C_f}{\phi . \varepsilon_o \varepsilon_r k_b T}} .$$

Eq. (14) and Eq. (19) show the dependence of the effective excess charge density on microstructure parameters of porous media (capillary radius, porosity, tortuosity and permeability) and electrokinetic parameters (ionic concentration, valence of ions and the zeta potential).

3. Results and discussion

In this work, a system of 1:1 symmetric electrolytes such as NaCl, KNO_3 (Z = 1) and silica-based surfaces are considered at room temperature (T=295 K) for the modeling because of the availability of input parameters. For silica-based rocks saturated by 1:1 symmetric electrolytes, the C_f - ζ relation is found to follow [26]:

$$\zeta = a + b\log_{10}(C_f) \tag{20}$$

where a = -9.67 mV, b = 19.02 mV (ζ in mV).

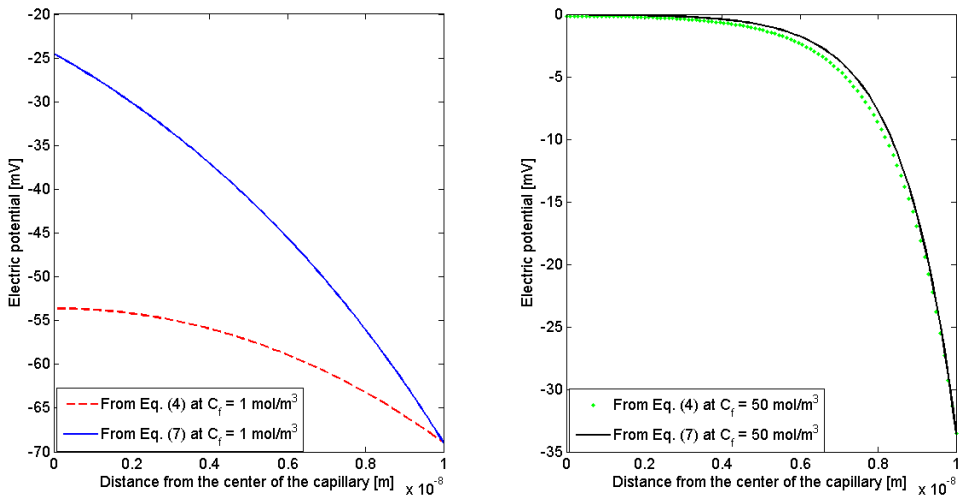

(a) (b)

Figure 3. The variation of the electric potential $\psi(r)$ with respect to distance r using Eq. (4) and Eq. (7) at C_f = 1 mol/m^3 (a) and C_f = 50 mol/m^3 (b).

The variation of the electric potential $\psi(r)$ with respect to distance r from the center of the capillary predicted from Eq. (4) and Eq. (7) at two different electrolyte concentrations of C_f = 1 mol/m^3 and C_f = 50 mol/m^3 is shown in Fig. 3 for the radius $R = 10^{-8}$ m. To get Fig.3, the values of λ and ζ calculated from Eq. (6) and Eq. (20) at C_f = 1 mol/m^3 and C_f = 50 mol/m^3 are 0.96×10^{-8} m, -69 mV and 0.13×10^{-8} m, -34 mV, respectively. It is shown that when the radius R is approximately the same as the Debye length λ at C_f = 1 mol/m^3, the electric potential predicted from Eq. (4) is much different from Eq. (7). However, the predictions from Eq. (4) and Eq. (7) are in good agreement with each other as expected when a thin EDL assumption is valid at C_f = 50 mol/m^3 (λ =0.13×10^{-8} m and $R/\lambda \approx 8$).

From Eq. (12), the dependence of the effective excess charge density $\hat{Q}_v^R$ on the capillary radius R at two different electrolyte concentrations of C_f = 1 mol/m^3 (a) and C_f = 50 mol/m^3 (b) is shown in Fig. 4 (the dash lines). It is seen that the effective excess charge density decreases with increasing capillary radius. Additionally, Guarracino and Jougnot (2018) obtained the effective excess charge density in a capillary $\hat{Q}_v^R$ and in a porous medium $\hat{Q}_v^{REV}$ after some approximations and under a thin EDL assumption as below [19]:

$$\hat{Q}_v^R = \frac{8N_A eC_f}{(R/\lambda)^2}\left[-2\frac{e\zeta}{k_bT} - \left(\frac{e\zeta}{3k_bT}\right)^3\right] \tag{21}$$

and

$$\hat{Q}_v^{REV} = N_A eC_f \lambda^2\left[-2\frac{e\zeta}{k_bT} - \left(\frac{e\zeta}{3k_bT}\right)^3\right]\frac{1}{\tau^2}\frac{\phi}{\kappa} \tag{22}$$

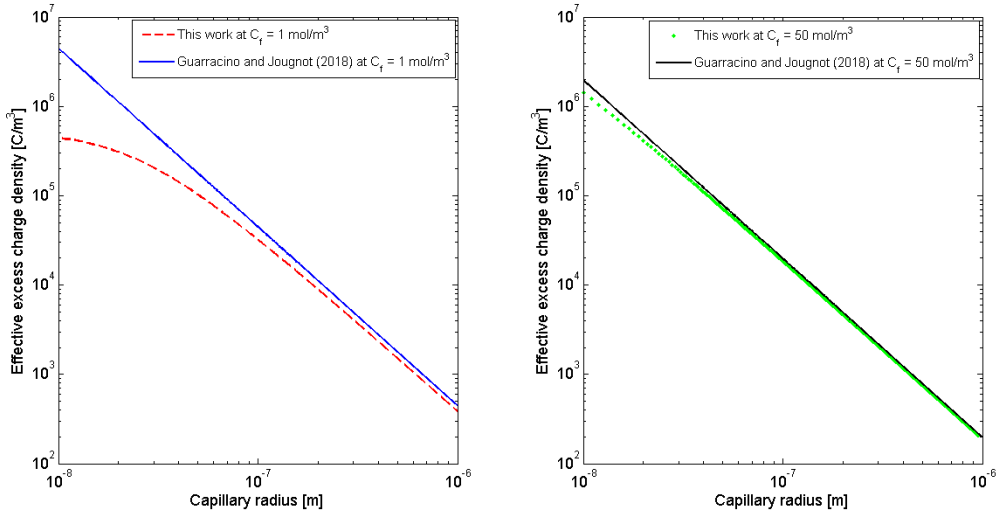

(a) (b)

Figure 4. Dependence of the excess charge density $\hat{Q}_v^R$ on the capillary radius R predicted from this work (the dashed lines) and from Guarracino and Jougnot (2018) (the solid lines) at C_f = 1 mol/m^3 (a) and C_f = 50 mol/m^3 (b).

The variation of the effective excess charge density $\hat{Q}_v^R$ with the capillary radius R predicted from Eq. (21) is also shown in Fig. 4 at the same electrolyte concentrations (the solid lines). It is found that the model of [19] always overestimates the effective excess charge density for any value of the capillary radius at both electrolyte concentrations. Similarly, the result shows that when the radius R is approximately the same as the Debye length λ at C_f = 1 mol/m^3, the effective excess charge density $\hat{Q}_v^R$ predicted from this work is far different from [19] as shown in Fig. 4a. However, values of $\hat{Q}_v^R$ predicted from this work and from [19] are almost the same as shown in Fig. 4b when a thin EDL assumption is valid at C_f = 50 mol/m^3 (R/ $\lambda \geq 8$). The ratio of R/ $\lambda \geq 8$ is in good agreement with the value of R/ $\lambda \geq 5$ when the thin EDL assumption is valid as reported in [19].

The predictions of the excess charge density $\hat{Q}_v^{REV}$ in the porous medium as a function of electrolyte concentration C_f and the permeability κ from this work and from [19] are shown in Fig. 5 and Fig. 6, respectively. Input parameters used for modeling in Fig. 5 are $\phi = 0.2$, $\tau = 1.95$, κ = 10^{-14} m^2 and in Fig. 6 are $\phi = 0.2$, $\tau = 1.95$, C_f = 1 mol/m^3. The reason to use the above parameters is that they have been used for modeling in [19]. Fig. 5 shows that the effective excess charge density $\hat{Q}_v^{REV}$ decreases with increasing electrolyte concentration. This is explained by the decrease of the EDL thickness when the electrolyte concentration increases [e.g., 11, 13, 14]. Consequently, the excess charge in the EDL and the effective excess charge density decrease. Fig. 6 shows that the $\hat{Q}_v^{REV}$ decreases with increasing permeability of porous media. This behavior is suitable with what is predicted in Fig. 4 because there is a link between the pore radius and permeability of porous media as shown in Eq. (18). Additionally, the results in Fig. 5 and Fig. 6 show that the model proposed by [19] overestimates the effective excess charge density at a given electrolyte concentration as well as permeability. The deviation between this work and [19] depends on the ratio of capillary/pore radius and the Debye length.

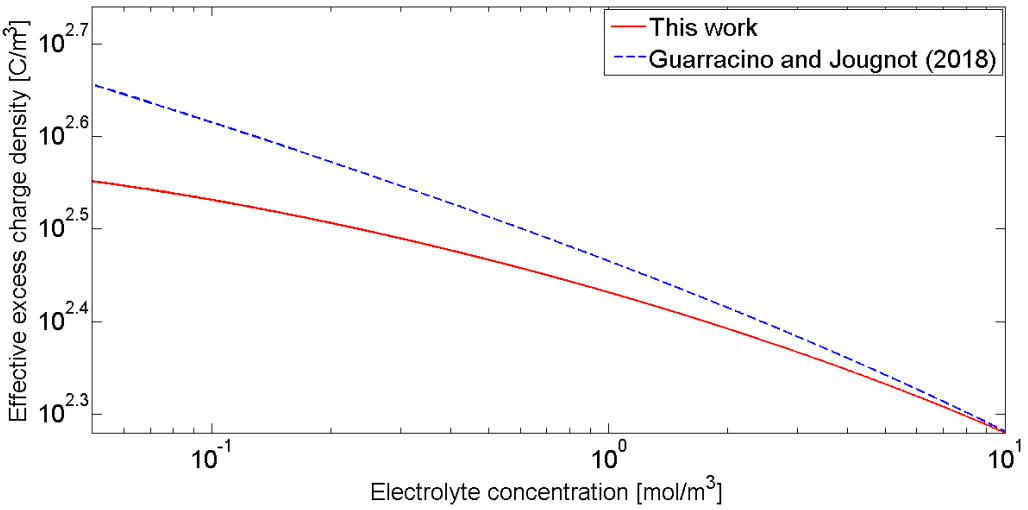

Figure 5. The variation the effective excess charge $\hat{Q}_v^{REV}$ with electrolyte concentration C_f predicted from this work (the dashed line) and from Guarracino and Jougnot (2018) (the solid line).

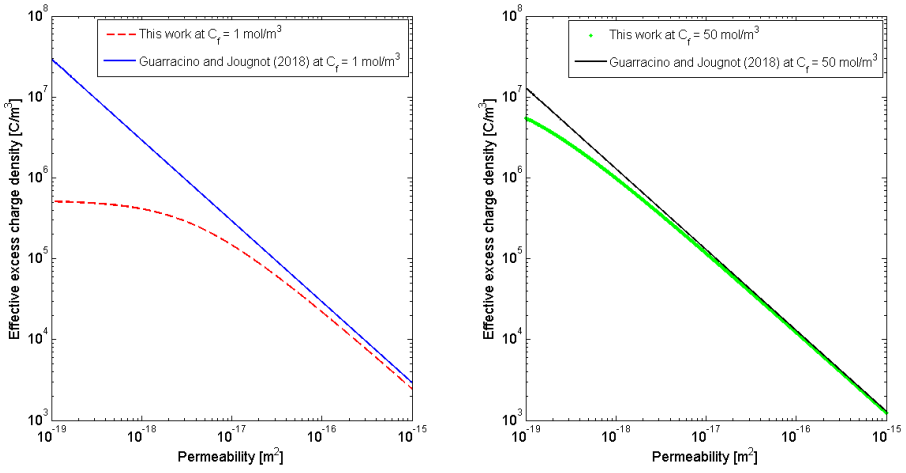

(a) (b)

Figure 6. The variation of the effective excess charge $\hat{Q}_v^{REV}$ with permeability κ predicted from this work (the dashed lines) and from Guarracino and Jougnot (2018) (the solid lines) at C_f = 1 mol/m^3 (a) and C_f = 50 mol/m^3 (b).

The reasons for a difference between this work and [19] are not only due to the thin EDL assumption to get $\psi(r)$ and $\rho(r)$ but also to approximations to evaluate integrals as performed by [19]. Namely, Guarracino and Jougnot (2018) applied Taylor series expansions of exponential functions and only used the first four terms [19]. They then used a thin EDL assumption again to simplify integrals. Therefore, those approximations lead to another deviation contributing to the difference between this work and

[19]. However, when the thin EDL assumption is valid (R/ $\lambda \geq 8$), the model proposed by [19] is in good agreement with the model obtained in this work for arbitrary pore scales.

4. Conclusion

In this work, a model for the effective excess charge in a capillary $\hat{Q}_v^R$ as well as in porous media $\hat{Q}_v^{REV}$ is developed for arbitrary pore scales. The results of $\hat{Q}_v^R$ and $\hat{Q}_v^{REV}$ as a function of the capillary radius, electrolyte concentration and permeability predicted from the obtained model are then compared with those from [19]. The comparisons show that the effective excess charge densities predicted from the model of [19] are always larger than those predicted from this work. The deviation between them depends on the ratio of capillary/pore radius and the Debye length R/λ. When the pore radius is approximately the same as the Debye length, there is a big difference between two models. However, when the ratio of R/λ is larger than 8, two models are in very good agreement with other. The possible reasons for a difference between two models are not only due to the thin EDL assumption to get $\psi(r)$ and $\rho(r)$ but also to some approximations for integral evaluations used in [19]. The results suggest that the obtained model is more general and can be used with arbitrary capillary/pore scale and thus is not restricted to the thin EDL assumption.

Acknowledgments

This research is funded by Vietnam National Foundation for Science and Technology Development (NAFOSTED) under grant number 103.99-2016.29.

References

[1] M. Aubert, Q.Y. Atangana, Groundwater, 34 (1996) 1010–1016.
[2] A. Finizola, J.-F. Lénat, O. Macedo, D. Ramos, J.-C. Thouret, F. Sortino, J. Volcanol. Geoth. Res., 135 (2004) 343–360.
[3] C. Doussan, L. Jouniaux, J.-L. Thony, Journal of Hydrology 267 (2002) 173–185.
[4] F. Perrier, M. Trique, B. Lorne, J.-P. Avouac, S. Hautot, P. Tarits, Geophys. Res. Lett. 25 (1998) 1955–1958.
[5] Martinez-Pagan, P., A. Jardani, A. Revil, and A. Haas, Geophysics 75 (2010) WA17–WA25.
[6] Naudet, V., A. Revil, J.-Y. Bottero, and P. Bgassat, Geophysical Research Letters 30 (2003).
[7] V. Naudet, M. Lazzari, A. Perrone, A. Loperte, S. Piscitelli, V. Lapenna, Engineering Geology 98 (2008) 156-167.
[8] A. Perrone, A. Iannuzzi, V. Lapenna, P. Lorenzo, S. Piscitelli, E. Rizzo, F. Sdao, Journal of Applied Geophysics 56 (2004) 17-29.
[9] Jouniaux, L., A. Maineult, V. Naudet, M. Pessel, and P. Sailhac, C. R. Geoscience 341 (2009).
[10] Revil, A., and A. Jardani, The Self-Potential Method: Theory and Applications in Environmental Geosciences, Cambridge University Press, 2013.
[11] Hunter, R., Zeta Potential in Colloid Science: Principles and Applications, Colloid Science Series, Academic Press, 1981.
[12] Leroy, P., and A. Revil, Journal of Colloid and Interface Science, 270 (2004) 371–380.
[13] T. Ishido, H. Mizutani, Journal of Geophysical Research 86 (1981) 1763-1775.
[14] P. W. J. Glover, E. Walker, M. Jackson, Geophysics 77 (2012) D17–D43.
[15] Revil, A., and P. Leroy, Journal of Geophysical Research 109 (2004).

[16] Linde, N., D. Jougnot, A. Revil, S. K. Matthäi, T. Arora, D. Renard, and C. Doussan, Geophys. Res. Lett. 34 (2007) L03306.
[17] Revil A. and Mahardika H, Water Resources Research 49 (2013) 744–766.
[18] Jardani, A., A. Revil, A. Bolève, A. Crespy, J. Dupont, W. Barrash and B. Malama, Geophysical Research Letters, 34 (2007) L24,403.
[19] L. Guarracino, D. Jougnot, Journal of Geophysical Research - Solid Earth 123 (2018) 52-65.
[20] Jackson M.D., Leinov E., International Journal of Geophysics 2012 (2012).
[21] Gierst L., J. Am. Chem. Soc. 88 (1966) 4768.
[22] Rice, C., and R. Whitehead, J. Phys. Chem. 69 (1965) 4017–4024.
[23] Pride, S., Physical Review B 50 (1994) 15,678–15,696.
[24] Bear, J., Dynamics of Fluids in Porous Media, Dover Publications, New York, 1988.
[25] Chan I. Chung, Extrusion of Polymers: Theory & Practice, Hanser-2nd edition, 2010.
[26] J. Vinogradov, M. Z. Jaafar, M. D. Jackson, Journal of Geophysical Research 115 (2010).